



**HAL**  
open science

## Impact of mechanical anisotropy on flat-rolled wires geometry

Thomas Massé, Yvan Chastel, Lionel Fourment, Pierre Montmitonnet,  
Christian Bobadilla, Nicolas Persem, Sylvain Foissey

► **To cite this version:**

Thomas Massé, Yvan Chastel, Lionel Fourment, Pierre Montmitonnet, Christian Bobadilla, et al.. Impact of mechanical anisotropy on flat-rolled wires geometry. 12th ESAFORM Conference on Material Forming, Apr 2009, Enschede, Netherlands. pp.Pages 363-366, 10.1007/s12289-009-0444-6 . hal-00509436

**HAL Id: hal-00509436**

**<https://hal-mines-paristech.archives-ouvertes.fr/hal-00509436>**

Submitted on 12 Aug 2010

**HAL** is a multi-disciplinary open access archive for the deposit and dissemination of scientific research documents, whether they are published or not. The documents may come from teaching and research institutions in France or abroad, or from public or private research centers.

L'archive ouverte pluridisciplinaire **HAL**, est destinée au dépôt et à la diffusion de documents scientifiques de niveau recherche, publiés ou non, émanant des établissements d'enseignement et de recherche français ou étrangers, des laboratoires publics ou privés.

# IMPACT OF MECHANICAL ANISOTROPY ON FLAT-ROLLED WIRES GEOMETRY

T. Massé<sup>1\*</sup>, Y. Chastel<sup>1</sup>, L. Fourment<sup>1</sup>, P. Montmitonnet<sup>1</sup>,  
C. Bobadilla<sup>2</sup>, N. Persem<sup>2</sup>, S. Foissey<sup>3</sup>

<sup>1</sup> Mines ParisTech, CEMEF - Centre for Material Forming, CNRS UMR 7635

<sup>2</sup> ArcelorMittal Gandrange, Research Center Long Carbon Bars & Wires

<sup>3</sup> ArcelorMittal Bourg-en-Bresse, Wire Solutions

**ABSTRACT:** A precise final geometry of flat-rolled wires is required in view of their industrial applications. However, comparison between experimental and computed cross-sections shows a gap of 10%. This difference might originate in the anisotropy introduced by wire drawing. Coefficients of an anisotropic constitutive model (Hill 48) have been identified from transverse compression tests. Then Lam3®, a finite element software, has been used to simulate rolling passes. The anisotropic law previously established significantly improves the estimation of the final width: yet the underestimation of the experimental width is 5% instead of 10%. Possible ways for further improvement are discussed.

**KEYWORDS:** High carbon steel, Wire drawing, Rolling, Anisotropy, Lateral spread, Hill criterion, Friction

## 1 INTRODUCTION

Flat-rolled steel wires are used e.g. in automotive industries. Since ever-higher mechanical characteristics and more complex geometries are required, the limits of the current forming processes tend to be reached. Numerical simulation may help improving the knowledge of the process. The manufacturing process involves wire drawing on single-pass benches followed by multi-pass tandem rolling, starting from a patented wire rod. In the past, some authors [1] have numerically shown that spread was quite sensitive to anisotropy; but no experimental results were shown. The present paper proves the effects of wire-drawing-induced mechanical anisotropy effects on flat-rolled wire width, a subject hitherto not addressed to the authors' knowledge. Here, the theoretical result in [1] is verified on a real material (high carbon steel) using its measured mechanical properties, therefore using physics-based simulation.

## 2 EFFECT OF ANISOTROPY

### 2.1 EVIDENCE OF ANISOTROPY

Following [2], the industrial drawing and flat-rolling process has been simulated by FEM (Forge2005®). Comparing experimental and computed final cross-sections, an important product characteristic in view of applications, a difference appears (Figure 1): the computed section is too narrow by  $\approx 10\%$ , way above the tolerance. This difference might originate in the anisotropy introduced by the wire drawing process, coming either from a crystallographic or a morphological texture (grain elongation). In the case of high carbon

steels, another probable origin is the progressive orientation of the pearlite colonies along the drawing axis, resulting also in the decrease of cementite interlamellar spacing [3-4]. The structure alignment is a major contribution to the development of a strong crystallographic texture [3-5]. All this explains the appearance and evolution of a strong anisotropy, as well as changes in the mechanical properties [3, 4, 6].

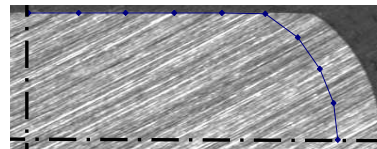


**Figure 1:** Comparison of experimental and computed (dark blue line) cross-sections

Plastic anisotropy can be easily manifested e.g. by ovalization in tension or compression tests [7, 8], since the difference in yield stress will favour one cross-sectional direction with respect to the other. In order to validate our hypothesis about anisotropy, compression tests in the transverse and longitudinal direction (Figure 2) have been performed at several stages of the drawing process. Figure 3 clearly shows a progressive ovalization for transverse samples, which confirms the appearance of anisotropy, more precisely an easier flow in the transverse (radial) as compared to the axial (drawing) direction. The yield stress shows a very weak 2% difference of between the two directions (Figure 5). In the longitudinal direction, no ovalization is visible (Figure 4), proving isotropy in the section. In the next paragraphs, the coefficients of an anisotropic constitutive model (Hill 48 [7]) will be identified from

\* Corresponding author: T. MASSÉ, CEMEF, BP 207,  
1 rue Claude Daunesse, 06904 Sophia Antipolis Cedex, France,  
Tel: (33)493957456, thomas.masse@mines-paristech.fr

the abovementioned compression tests. Then Lam3, a finite element software enabling to use Hill's plasticity, will be used to simulate rolling passes and to study the sensitivity of the process to anisotropy.

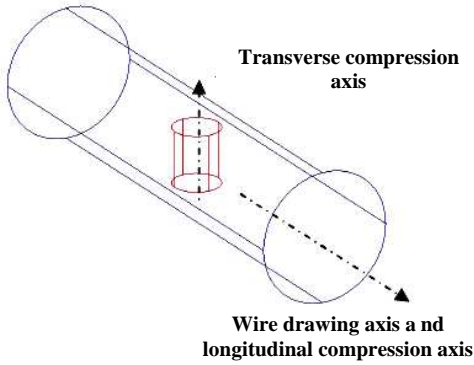


**Figure 2:** Scheme of transverse compression sampling

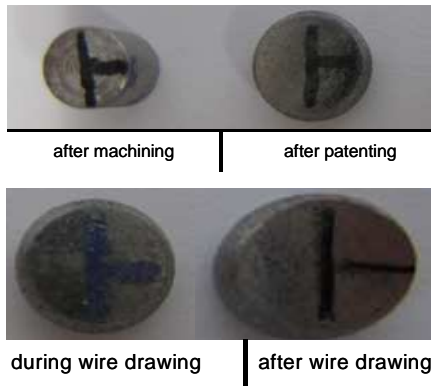


**Figure 3:** Compression tests in transverse direction highlight evolutive anisotropy. Initial dimensions are  $H = 6$  mm,  $R = 2.5$  mm. Height reduction 43%. The horizontal bar of the T is the radial direction; the vertical bar is the drawing direction.

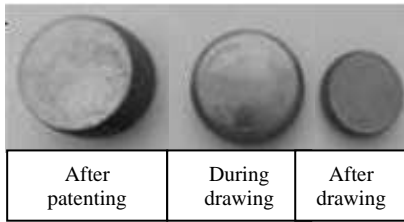


**Figure 4:** Compression tests in longitudinal direction highlight isotropic behaviour in the section. Height reduction 50%.

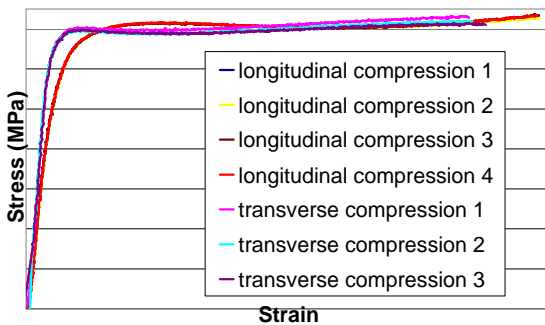


**Figure 5:** Compression stress-strain curves after drawing

## 2.2 ANISOTROPIC CONSTITUTIVE MODEL

The well-known isotropic, quadratic Von Mises criterion writes [9]:

$$\sigma_{eq}^2 = \frac{1}{2} [(\sigma_{yy} - \sigma_{zz})^2 + (\sigma_{zz} - \sigma_{xx})^2 + (\sigma_{xx} - \sigma_{yy})^2 + 6\sigma_{yz}^2 + 6\sigma_{zx}^2 + 6\sigma_{xy}^2] = \sigma_0^2 \quad (1)$$

To introduce anisotropy, Hill [7] kept the quadratic form, but added six coefficients to describe the direction-dependent plastic flow properties:

$$\left\{ F(\sigma_{YY} - \sigma_{ZZ})^2 + G(\sigma_{ZZ} - \sigma_{XX})^2 + H(\sigma_{XX} - \sigma_{YY})^2 + 2L\sigma_{YZ}^2 + 2M\sigma_{XZ}^2 + 2N\sigma_{XY}^2 \right\} = 1 \quad (2)$$

These parameters have a physical meaning, they are linked to the axial and shear yield stresses:

$$\sigma_{0XX} = \frac{1}{\sqrt{G+H}}, \quad \sigma_{0YY} = \frac{1}{\sqrt{F+H}}, \quad \sigma_{0ZZ} = \frac{1}{\sqrt{F+G}}, \quad (3)$$

$$\sigma_{0XZ} = \frac{1}{\sqrt{2M}}, \quad \sigma_{0XY} = \frac{1}{\sqrt{2N}}, \quad \sigma_{0YZ} = \frac{1}{\sqrt{2L}}$$

Thus, the equivalent stress can be chosen as [1]:

$$\sigma_{eq}^2 = A \cdot \left\{ \begin{array}{l} F(\sigma_{YY} - \sigma_{ZZ})^2 + G(\sigma_{ZZ} - \sigma_{XX})^2 \\ + H(\sigma_{XX} - \sigma_{YY})^2 \\ + 2L\sigma_{YZ}^2 + 2M\sigma_{XZ}^2 + 2N\sigma_{XY}^2 \end{array} \right\} \quad (4)$$

In the anisotropic case, A is taken by convention as [1]:

$$A = \frac{1}{2} \sqrt{\frac{3}{\Sigma}}, \quad \text{with } \Sigma = FH + FG + GH \quad (5)$$

$F=G=H=1$  and  $L=M=N=3$  return the Von Mises criterion (1). Hill's criterion therefore appears as the simplest quadratic generalization of Von Mises criterion. The axis-symmetry of drawing brings further simplification, since all directions in the cross section are equivalent:

$$H = G, \quad N = M, \quad L = 2F + G \quad (6)$$

Equation (2) becomes:

$$\sigma_{eq}^2 = A \cdot \left\{ \begin{array}{l} F(\sigma_{YY} - \sigma_{ZZ})^2 \\ + G[(\sigma_{ZZ} - \sigma_{XX})^2 + (\sigma_{XX} - \sigma_{YY})^2] \\ + 2M\sigma_{XZ}^2 \end{array} \right\} \quad (7)$$

## 2.3 COEFFICIENTS MEASUREMENT

Ovalization can be characterized by the shape factor of the section (Figure 6) and related to the anisotropy coefficients, giving a first relation from which F/G can be identified:

$$\frac{b}{a} = \left( \frac{h_0}{h} \right)^{(F-G)/(F+G)} \quad (8)$$

To fully identify the three coefficients F, G and M, more information is required. The yield stress in the transverse direction (equation (3) for  $\sigma_{0zz}$ ) gives G, and torsion tests give access to M. All the experimental stress – strain curves available for our material at all stages of the cold forming schedule have been compiled in Figure 7 (tensile tests, transverse and longitudinal compression tests). These curves lead to the coefficients reported in Table 1. Furthermore, a strain hardening law [2] can be identified from Figure 7, valid for all tests and deformation modes.

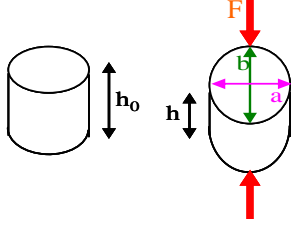


**Figure 6:** Compression test geometry

These parameters have been validated by re-simulating the compression tests. We first had to identify friction based on barrelling, resulting in a Tresca's friction factor  $\bar{m} = 0.2$ . Then, recomputing compression tests resulted in a good agreement on ovalization as shown in Figure 8 ( $b/a = 1.21$  instead of 1.24 experimentally).

But the agreement on the yield stresses is far from satisfactory. In the experiments, the difference between the axial and the radial yield stress is never more than 2%. Fitting ovalization and the radial yield stress as described above leaves us with a ratio  $\sigma_{0xx} / \sigma_{0rr} = 1.3$ . This difficulty is usual in sheet forming, where it is very hard to fit the angular dependence of both flow pattern (Lankford coefficient) and yield stress [10-12]. More sophisticated anisotropy models need be developed for this purpose [13]. In the absence of any reliable, widely accepted anisotropy model for bulk material (except maybe polycrystalline models [14-15]), and since we are firstly interested in transverse flow, the following study is carried out with the constitutive parameters identified above from the flow pattern in compression.

**Table 1:** Reduced parameters of anisotropic Hill criterion ( $\times 10^6 \text{ MPa}^{-2}$ ) during wire drawing

	Non-drawn	Half-drawn	Fully drawn
<b>F/G</b>	0.995	1.525	2.261
<b>L/M</b>	1	1.07	1.25

## 2.4 SIMULATION OF ROLLING WITH ANISOTROPY

Here, the simulation is running with the above anisotropic behaviour law, associated to an EVP formulation and Hill's parameters obtained at the end of wire drawing. We keep the same values all along rolling. Lam3 works in stationary mode with linear hexahedral elements with 8 Gauss points. We use a Tresca friction law writing:

$$\tau_c = \bar{m} \frac{\sigma_0}{\sqrt{3}}, \quad \text{with } \bar{m} = 0,2 \quad (10)$$

The simulation takes into account tensions between rolling stands. A more precise description of geometry, computing conditions and kinematics is giving in [2]. Sections shown below are those of the last rolling pass.

As shown in Figure 9, rolling simulation with the anisotropic law previously established significantly improves the estimation of the final width in terms of widening: yet the underestimation of the experimental width is 5% instead of 10%. As mentioned above, Hill's quadratic criterion is not sufficient to describe our bulk material anisotropy.

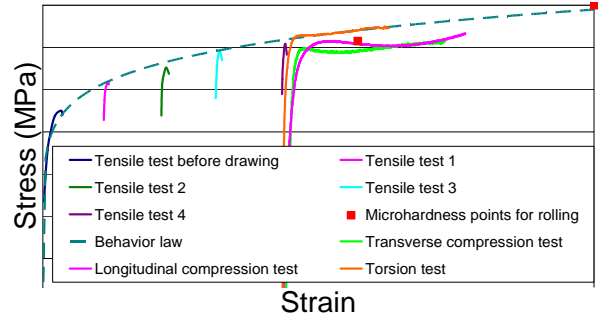


**Figure 7:** Strain-stress curves at all stages of the cold forming process (scales withdrawn for confidentiality)

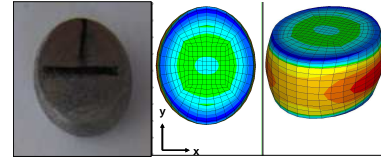


**Figure 8:** Comparison between experimental and numerical ovalization

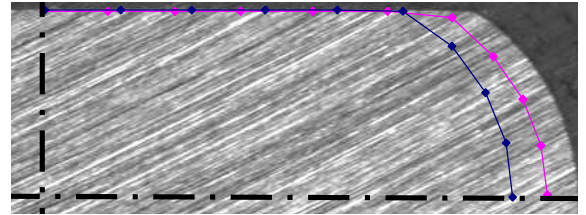


**Figure 9:** Comparison of experimental and computed (blue line for isotropic law and pink line for anisotropic law) cross-sections

This is why this analysis has been complemented with two parametric sensitivity studies. The first one deals with anisotropy factors, namely the radial / axial yield stress ratio and the shear yield stress / mean tensile yield stress (Table 2): width strongly depends on the ratios between F, G and H, while L, M and N affect mainly the side barrelling (Figure 10).

The second study is about friction. In the Lam3 FEM software, an anisotropic friction law is available. It is based on a velocity-dependent Coulomb model:

$$\tau_{X(respY)} = \text{Min}(\mu_{X(respY)} \cdot \sigma_n, m_{X(respY)} \cdot K \cdot v_g^p) \quad (11)$$

where  $r = \frac{\mu_x}{\mu_y}$  is the ratio of friction coefficients in the X

and Y directions.  $r > 1$  penalizes the flow in the longitudinal direction and therefore enhances transverse flow. Figure 11 shows that the isotropic friction coefficient has no notable impact on widening (default value of friction factor  $m$  is 0,2). Anisotropic friction ( $r=2$ ) expectedly increases spread, but the width under-estimation decreases only from 5% to 4%: friction does not explain the too small computed widening.

**Table 2: Parameters of anisotropic Hill criterion**

$\frac{\sqrt{2G}}{\sqrt{F+G}} = \frac{\sigma_{yy}}{\sigma_{xx}}$	$\frac{\sqrt{F+G} + \sqrt{G+H} + \sqrt{F+H}}{\sqrt{2L} + \sqrt{2M} + \sqrt{2N}} \equiv \frac{\tau}{\sigma}$	Widening
1	$1/\sqrt{3} = 0.577$	90%
0.78	0.541	94.5%
0.78	0.427	94.2%
0.78	0.27	95%
0.78	0.171	96.3%
0.53	0.577	98.2%

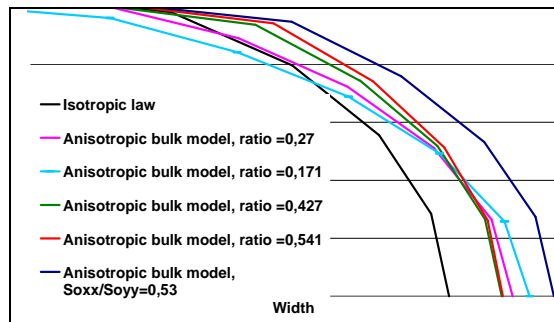


**Figure 10: Sensitivity of computed cross-sections to Hill's parameters**

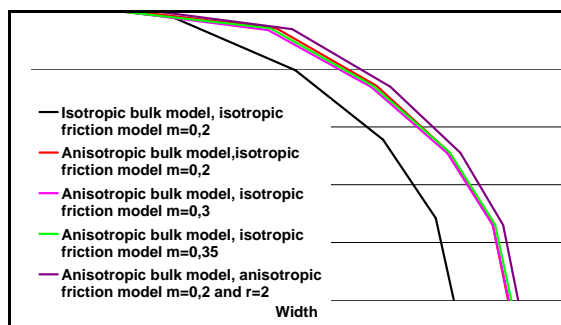


**Figure 11: Sensitivity of computed cross-sections to anisotropic friction parameter**

### 3 CONCLUSIONS

The role of anisotropy has been emphasized in flat wire cold rolling by comparison with experiments. Further studies have to be carried out to correctly and accurately predict final cross-sections. More precise material modelling would be necessary for this purpose, such as, by order of growing complexity:

- Re-measuring Hill's parameters after the rolling process, whereas they were constant in this work;

- Using a more complex phenomenological anisotropic law (Hosford [11], Barlat [13]...);
- Using micro-macro modelling based on lamellar microstructure (rather than polycrystalline models [14, 15] in the present case): its progressive orientation has been shown to explain mechanical anisotropy [16].

### REFERENCES

- [1] P. Montmitonnet, P. Gratacos, R. Ducloux. Application of anisotropic viscoplastic behaviour in 3D finite-element simulations of hot rolling. *J. Mat. Process. Technol.*, 53 (3-4):662-683, 1995.
- [2] C. Bobadilla, N. Persem, S. Foissey, Modelling of the drawing and rolling of high carbon flat wires. In *AIP Conference*. 907:535-540, 2007.
- [3] J.D. Embury, R.M. Fisher. The structure and properties of drawn pearlite. *Acta Met.* 14:147-159, 1966.
- [4] G. Langford. Deformation of pearlite. *Met. Trans.* 8A:861-875, 1977.
- [5] M. Zelin. Microstructure evolution in pearlitic steels during wire drawing. *Acta Mat.* 50:4431-4447, 2002.
- [6] B. Devincere, T. Hoc, L. Kubin. Dislocation mean free path and strain hardening of crystals. *Science* 320:1745-1748, 2008.
- [7] R. Hill. A theory of the yielding and plastic flow of anisotropic metals. In *Proc. Royal Soc. Of London*. A193:281-297, 1948.
- [8] A. Gaillac. *Endommagement d'alliages de zirconium - Impact sur la laminabilité*, PhD Thesis, SIMaP-INPG (2007). In French.
- [9] Von Mises, R. Mechanik der plastischen Formmnderung von Kristallen. *Z. Angew Math. Mech.* 8:161-185, 1928.
- [10] M. Ben Tahar. *Contribution à l'étude et la simulation du procédé d'hydroformage*. PhD thesis, CEMEF - ENSMP, (2005). In French.
- [11] W.F. Hosford, R.M. Caddell. *Metal Forming - Mechanics and Metallurgy*. 2<sup>nd</sup> ed. (1993). Prentice Hall Inc. USA.
- [12] R.W. Logan, D.J. Meuleman, W.F. Hosford. The effects of anisotropy on the limiting drawing ratio. In *TMS-AIME Conference*, 159-173, 1986.
- [13] F. Barlat. Crystallographic texture, anisotropic yield surfaces and forming limits of sheet metals. *Mater. Sci. Engg.* 91:55-72, 1987.
- [14] G. Proust, C.N. Tomé, G.C. Kaschner. Modeling texture, twinning and hardening evolution during deformation of hexagonal materials. *Acta Mat.* 55:2137-2148, 2007.
- [15] F.D. Fischer, H. Clemens, T. Schaden and F. Appel. Compressive deformation of lamellar microstructures - a short review. *Int. J. Mat. Res.* 98:1041-1046, 2007.
- [16] A. Milenin, Z. Muskalski. Multi-scale FEM simulation of the drawing process. *Comp. Meth. Mat. Sci.* 7:156-16, 2007.